The *End2* Mutation in CHO Cells Slows the Exit of Transferrin Receptors from the Recycling Compartment but Bulk Membrane Recycling Is Unaffected

John F. Presley, Satyajit Mayor, Kenneth W. Dunn, Lester S. Johnson, Timothy E. McGraw, and Frederick R. Maxfield

Department of Pathology, Columbia University College of Physicians and Surgeons, New York, New York 10032

Abstract. We have characterized a new CHO cell line (12–4) derived from a parental line, TRVb-1, that expresses the human transferrin receptor. This mutant belongs to the *end2* complementation group of endocytosis mutants. Like other *end2* mutants, the endosomes in 12-4 cells show a partial acidification defect. These cells internalize LDL and transferrin at 70% of the rate of parental cells and externalize transferrin at 55% of the parental rate (Johnson, L. S., J. F. Presley, J. C. Park, and T. E. McGraw. *J. Cell Physiol.* 1993). In this report, we have used fluorescence microscopy to determine which step in receptor trafficking is affected in the mutants. Transferrin is sorted from LDL and is delivered to a peri-centriolar recycling compartment at rates similar to parental cells. However, the rate constant for exit of transferrin from the recycling compartment in mutant cells is 0.025 min^{-1} vs 0.062 min^{-1} in the parental line. We also measured the trafficking of a bulk membrane marker, 6-[*N*-[7-nitrobenzo-2-oxa-1,3-diazol-4-yl]-amino]hexanoyl-sphingosylphosphorylcholine (C_6-NBD-SM) that labels the exofacial side of the plasma membrane. C_6-NBD-SM enters the same recycling compartment as transferrin, and it exits the recycling compartment at a rate of 0.060–0.065 min^{-1} in both parental and 12–4 cells. We conclude that bulk membrane flow in the recycling pathway of 12–4 cells is normal, but exit of transferrin from the recycling compartment is slowed due to retention in this compartment. Thus, in the mutant cell line the recycling compartment carries out a sorting function, retaining transferrin over bulk membrane.

TRANSFERRIN (Tf)[1] recycling requires passage through a series of endosomal compartments (McGraw and Maxfield, 1990). After internalization via coated pits, Tf and other ligand-receptor complexes are delivered to early sorting endosomes, which are acidic organelles. The low pH in these early sorting endosomes causes dissociation of LDL and many other ligands from their receptors (Maxfield and Yamashiro, 1991). The low pH also causes conversion of diferric Tf to apo-Tf which remains bound to the transferrin receptor (Tf-R) until exposure to neutral pH at the cell surface (Harford et al., 1991). Tf is rapidly removed from these sorting endosomes while LDL and other lysosomally targeted ligands are retained and accumulated. After removal from the sorting endosomes, Tf is found in a recycling compartment which contains other recycling receptors (McGraw et al., 1993) but does not contain significant amounts of lysosomally targeted molecules such as LDL or α_2-macroglobulin (Yamashiro et al., 1984; Dunn et al., 1989). In CHO cells this recycling compartment, which is composed of narrow diameter tubules (Yamashiro et al., 1984), concentrates near the microtubule organizing center. Many of the receptors (including the Tf-R and LDL receptor), and most of the membrane lipids are efficiently recycled back to the cell surface (Goldstein et al., 1985; Koval and Pagano, 1989; Mayor et al., 1993). While general features of the endocytic pathway are becoming known, many of the mechanisms controlling endocytic trafficking remain undetermined. Even the functions of some organelles, such as the recycling compartment, are essentially unknown. Does it sort, or is it a passive reservoir for return of molecules to the cell surface?

Studies involving the selection of a panel of mutants organized into complementation groups, and further analysis using a combination of genetic and biochemical techniques have been highly successful in the study of membrane traffic in yeast (Novick et al., 1980, 1981; Newman and Ferro-Novick, 1990; Hicke and Schekman, 1990). Thus far, the genetic approaches have proved less informative in mammalian cells. The primary difficulties have been in selection of mutants defective in vesicular trafficking pathways, and in

1. *Abbreviations used in this paper*: Tf, transferrin; Tf-R, transferrin receptor; C_6-NBD-SM, 6-[*N*-[7-nitrobenzo-2-oxa-1,3-diazol-4-yl]-amino]hexanoyl-sphingosylphosphorylcholine; C_6-NBD-Cer, 6-[*N*-[7-nitrobenzo-2-oxa-1,3-diazol]] aminocaproyl sphingosine; LDL, low density lipoprotein; DiI, 3,3′-dioctadecylindocarbocyanine; DiO, 3,3′-dioctadecyloxacarbocyanine; TxR, Texas Red; R-F-Tf, rhodamine-fluorescein transferrin.

detailed characterization of the few endocytosis mutants that do exist (Cain et al., 1991; Colbaugh et al., 1988; Robbins et al., 1983).

A selection scheme using a parental CHO cell line, TRVb-1 (McGraw et al., 1987) that expresses only the transfected human Tf-R yielded a new member of the *end*2 complementation group defective in endosomal functions (Johnson et al., 1993). *End*2 mutants (Roff et al., 1986) have been shown to have defects in acidification of some endosomes (Schmid et al., 1989; Yamashiro and Maxfield, 1987), and in other aspects of vesicular trafficking (Robbins et al., 1984). The properties of the transfected human Tf-R facilitated a more detailed analysis of the recycling kinetics in 12–4 cells than had been done in *end*2 mutants carrying the hamster receptor. This analysis showed that Tf-R recycling was ~twofold slower in 12–4 cells than in the parental cells. This slowing was then detected in other mutants of the *end*2 group (Johnson et al., 1993).

In this study, we used fluorescence microscopy and digital image analysis to determine which portions of the recycling pathway are defective in the mutant 12–4 cell line. Sorting from LDL, transit to the recycling compartment, and exit from the recycling compartment were all measured using fluorescent Tf as a tracer. Additionally, the pleiotropic nature of the mutants was investigated by comparing the trafficking of a bulk membrane marker, 6-[*N*-[7-nitrobenzo-2-oxa-1,3-diazol-4-yl]-amino]hexanoyl-sphingosylphosphorylcholine (C_6-NBD-SM), in the parental and mutant cells. These studies identified exit from the recycling compartment as the affected step in Tf recycling and showed that C_6-NBD-SM recycling was unaffected in these cells.

Materials and Methods

All chemicals were from Sigma Chemical Company (St. Louis, MO) unless otherwise stated. Tissue culture supplies were from Gibco Laboratories (Grand Island, NY), except for plasticware, which was from Falcon (Becton Dickinson, Oxnard, CA). Chromatography grade butanol, chloroform, 30% ammonium hydroxide, and methanol were from EM Science (Gibbstown, NJ). Silica 60 high performance chromatography plates were from E. Merck (Darmstadt, FRG).

Fluorescent Probes

Fluorescent DiI and DiO LDLs (Tabas et al., 1990) were provided by Drs. Jeffrey Myers and Ira Tabas (Columbia University, New York, NY). 6-[*N*-[7-nitrobenzo-2-oxa-1,3-diazol]] aminocaproyl sphingosine (C_6-NBD-Cer) and 6-[*N*-[7-nitrobenzo-2-oxa-1,3-diazol-4-yl]-amino]hexanoyl-sphingosylphosphorylcholine (C_6-NBD-SM) were purchased from Molecular Probes, Inc. (Eugene, OR).

Human Tf was iron loaded, and purified by Sephacryl S-300 gel filtration before use. Tf was conjugated to TRITC or FITC as described in Yamashiro et al. (1984). Succinimidyl ester of Texas Red (TxR) was purchased from Molecular Probes, Inc. and conjugated to Tf according to manufacturer's instructions. For pH measurements transferrin conjugated with both rhodamine and fluorescein was prepared by reacting transferrin with succinimidyl esters of both carboxytetramethylrhodamine and carboxyfluorescein according to the manufacturer's instructions (Molecular Probes, Inc.) in a ratio of 8 mg Tf to 0.7 mg carboxyfluorescein to 0.22 mg carboxytetramethylrhodamine. Cells incubated with this double-labeled conjugate (F-R-Tf) showed brightly labeled endosomes in a pattern characteristic of transferrin in TRVb-1 cells. F-R-Tf labeling was receptor mediated and the trafficking kinetics were similar to singly labeled Tf: the F-R-Tf was recycled and released by cells during an ensuing chase period in the presence of 0.5 mg/ml unlabeled Tf and 10 μM deferoxamine. Labeling was inhibited in the presence of excess unlabeled transferrin.

Cells and Cell Culture

CHO derived cell lines, TRVb-1 (McGraw et al., 1987) and 12–4 (Johnson et al., 1993) were grown in bicarbonate buffered Hams F-12 medium supplemented with 5% FCS, and 2 g/l glucose in a humidified incubator in 5% CO_2 at 34°C. Cells were plated in coverslip bottom dishes (Saltzman and Maxfield, 1989) 2–3 d before microscopic observation.

Uptake of Fluorescently Labeled Tf and LDL

Immediately before labeling, cells grown in coverslip bottom dishes were washed with medium 1 (150 mM NaCl, 20 mM Hepes, pH 7.4, 1 mM $CaCl_2$, 5 mM KCl, 1 mM $MgCl_2$, 2 g/l glucose). Cells were then incubated in Hams F-12 medium containing 2 mg/ml ovalbumin, as described (Dunn et al., 1989). In all experiments in which DiI-LDL was used, LDL receptors were upregulated by incubating coverslip dishes in medium containing 5% delipidated serum (Goldstein et al., 1983) for 16–18 h before fluorescent labeling of the cells.

In experiments in which efflux of Tf from the recycling endosomes was measured, cells in coverslip bottom dishes were labeled continuously for 1 h with a fluorophore-Tf conjugate (FITC-Tf, TRITC-Tf, TxR-Tf or a mixture) at 37°C to reach a steady state or near steady state distribution of fluorescent Tf in the endocytic recycling pathway. The pulse was terminated with two washes in mild acid buffer (50 mM [*n*-morpholino]ethanesulfonic acid, 280 mM sucrose, pH 5.0, 37°C), and four washes in medium 1. The cells were then incubated at 37°C in chase medium (Hams-F12 containing 20 μM deferoxamine and 2 mg/ml ovalbumin) for various periods of time. At the end of the chase, cells were rinsed twice in mild acid wash, and then rinsed four times with medium 1, and fixed in 3.7% formaldehyde in medium 1 for 2 min. For short pulse-chases, in which sorting of Tf and LDL were examined, the cells were pulsed with a mixture of 20 μg/ml Tf and 5 μg/ml DiI-LDL, and chased as above. However, these incubations were done on a warm tray instead of in an incubator, and the incubation medium was bicarbonate-free Hams F-12, buffered to pH 7.4 with 20 mM Hepes.

pH Measurements

Cells were plated 2 d before each experiment onto 35-mm coverslip-bottom dishes. Tf-R expression levels of 12–4 cells and TRVb-1 cells were matched by culturing 12–4 cells in Ham's F-12 medium and TRVb-1 cells in McCoy's 5A medium, which lacks iron salts and thus causes an upregulation of Tf-R in TRVb-1 cells. Similar results were obtained when both cell lines were cultured in F-12.

Experimental dishes were preincubated in medium 1 for 20–30 min, then incubated in this same medium containing 20 μg/ml F-R-Tf for 10 or 30 min at 37°C on a bench-top warm tray. Fluorescent labeling was continued for approximately another 10 min on the microscope stage of a Zeiss Axiovert microscope warmed to 37°C during which time fluorescence images of the cells were collected by means of a Bio-Rad MRC-600 confocal attachment. The optical filters used to image rhodamine and fluorescein fluorescence were modified in order to optimize the detection of dimly fluorescent endosomes and the sensitivity to pH differences. In this modified system, 488 nm light is used to excite both fluorescein and rhodamine fluorescence. Fluorescein emissions (using a 515–545-nm bandpass filter), and rhodamine emissions (using a 600-nm long-pass filter) (Omega Optical Inc., Brattleboro, VT) were collected in the two Bio-Rad imaging detectors simultaneously. Using image processing techniques developed previously (Maxfield and Dunn, 1990), endosome fluorescence was quantified, and the ratio of red to green fluorescence was calculated for each endosome. For each experiment, calibration curves were constructed by imaging fixed, labeled cells which had been equilibrated with a series of pH buffers. One such calibration curve is shown in Fig. 7 *A*, which shows that the fluorescence emission ratio of the endocytic compartments labeled with F-R-Tf is a sensitive indicator of pH over a range from 5.0 to 7.0. Control experiments verified that the confocal detection system effectively eliminates the out-of-focus fluorescence of the medium.

C_6-NBD-SM Labeling of Recycling Compartment

Labeling of cells with C_6-NBD-SM was carried out as described elsewhere (Koval and Pagano, 1989; Mayor et al., 1993). Briefly, small unilamellar vesicles were made from C_6-NBD-SM and dioleylphosphatidylcholine (1:1) and incubated with cells at 2.5–5 μM C_6-NBD-SM concentration for 30 min at 2–4°C. In experiments where fluorescent-Tf and C_6-NBD-SM were measured by quantitative fluorescence microscopy, 25 μg/ml Texas-

Red-labeled Tf (Tx-Tf) was included in the labeling solution and the pulse-incubation medium. The cells were washed five times with Hams F-12 and incubated at 34–37°C for the indicated periods with prewarmed Hams F-12 to allow internalization of C_6-NBD-SM. The cells were then rapidly cooled with ice cold medium 1 and the C_6-NBD-SM on the cell surface was back-exchanged with six washes of 5% BSA in ice cold medium 1. Each wash was for 10 min at 0°C. Typically, this back exchange removed greater than 98–99% of surface associated lipid. After the back-exchange procedure the cells were incubated in chase medium (medium 1 containing 1% BSA) at 37°C to allow further endocytic processing and recycling. 20 μM deferoxamine was included in the chase medium in the experiments where Tx-Tf was used. For quantitative microscopic analyses, the cells were rinsed in ice-cold PBS and fixed in 2.5% paraformaldehyde in PBS for 30 min.

For biochemical analyses of potential C_6-NBD-SM metabolites (C_6-NBD-Cer and C_6-NBD-glucosylceramide) the chase medium was removed and lipid was extracted from it with an equal volume of *n*-butanol. The monolayers were rinsed with ice cold medium 1 and then were back exchanged with ice cold medium 1 containing 1% BSA for 15 min on ice. This back exchange medium was similarly butanol-extracted, and the extract was pooled with the butanol-extracted chase medium. (Less than 20% of the chase-medium fluorescence was recovered from the back-exchange medium.) The cells were washed twice at 0°C in ice cold PBS containing 5 mM EDTA (omitting Ca^{2+} and Mg^{2+}) and incubated for 5 min on ice in the same buffer. Cells were then removed by scraping with a rubber policeman, and the cell-associated lipids were extracted into an equal volume of butanol. The C_6-NBD-lipids were purified by TLC and quantified by spectrofluorometry (see below).

In the experiments shown in Fig. 6, C_6-NBD-lipids were directly quantified from the chase medium by fluorometric analysis of the butanol-extract of an aliquot of the chase medium withdrawn at different times. For the quantitative analysis shown: (*a*) total lipid was calculated as follows: total lipid = cell-associated fluorescence + fluorescence in remaining medium + fluorescence in chase aliquots; (*b*) fraction of the total lipid in the chase medium, *f*, at each time point was determined as follows: f = [10 × (lipid in chase aliquot) + lipid removed in previous chase aliquots]/total lipid; (*c*) fraction of lipid that was cell associated = $1 - f$.

NBD-Lipid Quantification

Butanol extracts were evaporated in vacuo in microcentrifuge tubes, and the pellet was resuspended in 25 μl $CHCl_3/CH_3OH$ (2:1; vol/vol). This was applied to a pre-baked (80°C, vacuum oven) Silica 60 high performance thin layer chromatography plate and allowed to air-dry. NBD-labeled standards (C_6-NBD-SM and C_6-NBD-Cer) were also applied in marker lanes, and the chromatogram was developed in a solvent system consisting of chloroform/methanol/30% NH_4OH/H_2O (350:150:18:7; vol/vol). The NBD-lipids were visualized under ultraviolet illumination. The areas corresponding to relevant NBD-labeled lipid (or NBD-labeled standard where the amount of lipid present in the sample was too faint to be visualized) were scraped, and the fluorescent lipid was extracted twice from silica into 400 μl chloroform/methanol/H_2O (4:4:1; vol/vol). NBD fluorescence was quantified on an SLM 8000 spectrofluorometer (SLM instruments, Urbana, IL) using an excitation wavelength of 470 nm, by integrating fluorescence emitted during a scan from 520 to 550 nm. In some experiments (Fig. 6) NBD fluorescence in the butanol-extracts was directly quantified without TLC.

Quantitative Fluorescence Microscopy

Measurement of the rate of Tf exit from the recycling compartment was conducted as follows. Cells on coverslip bottom dishes were labeled with a mixture of FITC-Tf (10 μg/ml) and TRITC-Tf (10 μg/ml) (both of known specific fluorescence) for 1 h to achieve steady state labeling of the recycling compartment. The cells were chased in the presence of FITC-Tf (20 μg/ml) alone, rinsed and fixed. Images were collected using a Leitz Diavert microscope (E. Leitz, Inc., Rockleigh, NJ) with a 40× objective, selective filter sets, and an image intensified video system (Videoscope, Washington, DC) as described previously (Dunn et al., 1989). Images were digitized from video tape using a digital time base corrector (I. Den Videotronics, New Britain, CT), and processed on a Vicom IP 8000 or 9000 image processor (Vicom, Fremont, CA) using a MicroVAXII host computer (Digital Equipment Co., Maynard, MA) and the LIPS set of image processing routines (Vicom, Fremont, CA).

The image processing methods used to identify and measure the fluorescence power of recycling compartments have been described elsewhere (Dunn et al., 1989; Saltzman and Maxfield, 1988; Yamashiro et al., 1984; Maxfield, 1989). Background was defined as the image remaining after a median filter operation using a neighborhood size of 128 × 128 pixels (33 × 33 μM). This median image was subtracted from the original image to give a background-corrected image. The validity of this background and thresholding method was checked as described elsewhere (Maxfield, 1989). After background correction, the recycling compartment was identified as a large area of fluorescence (>50 pixels) above a threshold of 10 intensity units (out of 255). For each of these areas, all contiguous pixels with a value greater than one third the value of the brightest pixel in the spot were retained as described by Dunn et al. (1989). The area of the recycling compartment was determined separately for the rhodamine and fluorescein labeled images, and the total recycling compartment was the union of these two spots. By visual inspection, spots larger than 50 pixels reproducibly corresponded to recycling compartments. The width of one pixel was equivalent to 0.26 μm when a 40× objective was used with the video camera. Rhodamine and fluorescein powers in the recycling compartment were calculated by summing the intensity values for each spot from precisely the same areas.

Fluorescence intensity values were corrected to compensate for the specific fluorescence of the two Tf conjugates as measured using the same microscope, objective lens, and video camera. This corrected fluorescence was used to measure mole fraction of receptors occupied by TRITC-Tf in the recycling compartments. The total corrected fluorescence (FITC + TRITC) was constant during the course of an experiment. Mole fraction was calculated on a cell-by-cell basis, and the values for cells from the same dish were averaged. At least 30 cells in 5–10 fields per dish were counted, and values obtained from three duplicate dishes on different days were aver-

Table I. Rate Constants for Transferrin and Lipid Recycling in Parental and Mutant Cells

Experiment	TRVb-1 (Parental) k_e	$t_{1/2}$	12-4 (Mutant) k_e	$t_{1/2}$
	(min^{-1}*)	(*min*)	(min^{-1})	(*min*)
Efflux of ^{125}I-TF after labeling to steady state‡	0.071 ± 0.001 (n = 2)	9.8	0.039 ± 0.002 (n = 2)	17.8
Efflux of TRITC-Tf from peri-centriolar recycling compartment§	0.062 ± 0.014 (n = 3)	11.2	0.025 ± 0.001 (n = 3)	27.7
Efflux of C_6-NBD-SM from cells‖	0.060 ± 0.0135 (n = 4)	11.6	0.0645 ± 0.01 (n = 4)	10.7
Efflux of C_6-NBD-SM from peri-centriolar recycling compartment	0.073¶ (n = 2)	9.5	0.074 ± 0.012** (n = 2)	9.4

* Rate constants for efflux, k_e, assuming first order kinetics. Values are mean ± SD.
‡ Johnson et al., 1993.
§ From Fig. 3.
‖ From data in Fig. 6.
¶ Mayor et al., 1993.
** From data in Fig. 5.

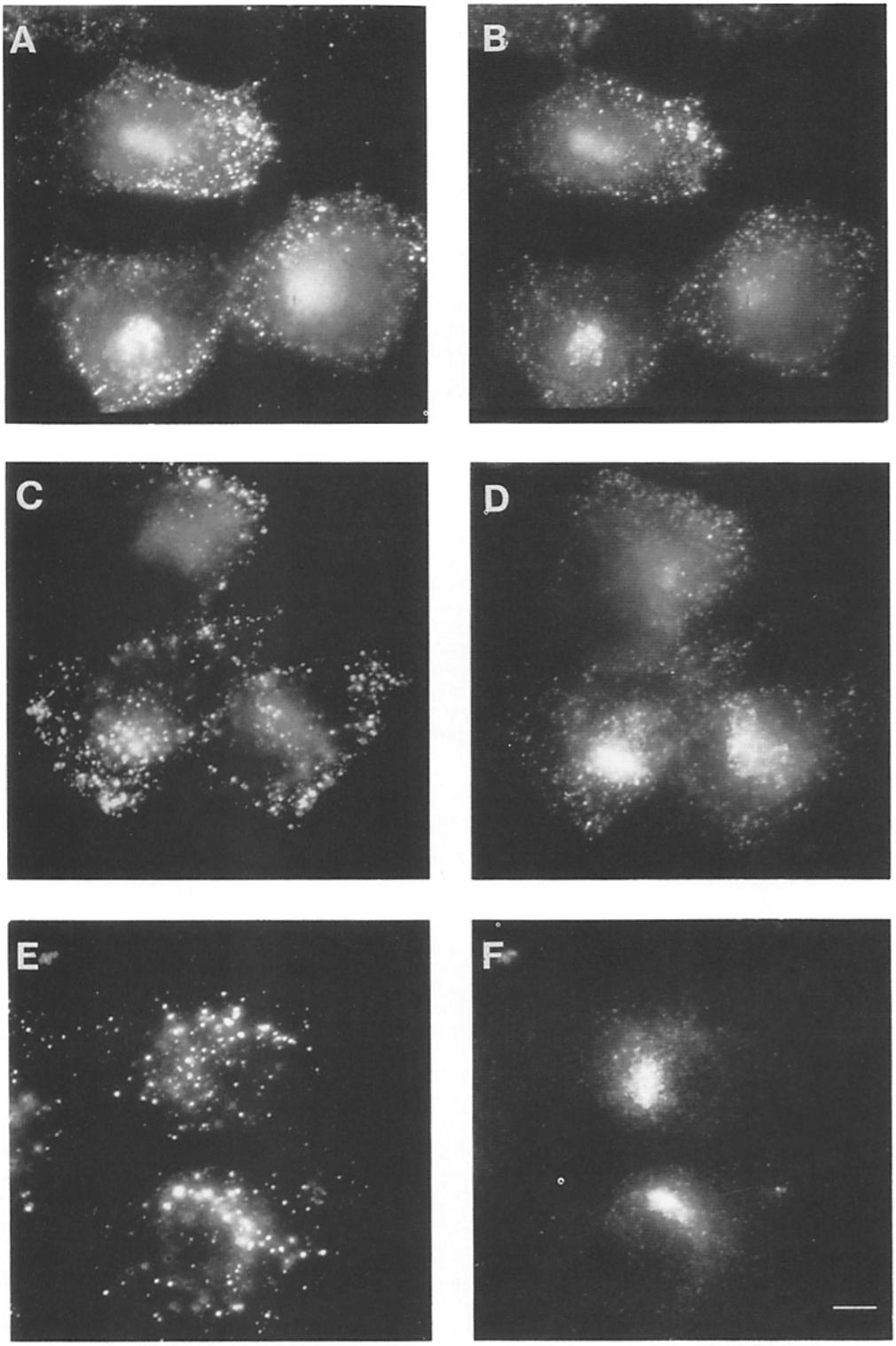

Figure 1. Sorting of Tf from LDL in mutant cells. 12–4 cells were labeled with FITC-Tf (20 μg/ml) and DiI-LDL (5 μg/ml) as described in Materials and Methods and then chased in the absence of label for the indicated times. Cells were fixed, and images were obtained using a cooled CCD camera and a 63× objective. (*A*, *C*, *E*) DiI-LDL. (*B*, *D*, *F*) FITC-Tf. *A* and *B* were labeled for 2 min with DiI LDL and FITC-Tf, and fixed. *C* and *D* were labeled for 2 min and chased for 4 min. *E* and *F* were labeled for 2 min and chased for 8 min. Bar, 10 μm.

aged for each time point. Rate constants for loss of TRITC-Tf were determined using the first 45 minutes of chase, assuming first order kinetics.

Pairs of C_6-NBD-SM and Tx-Tf images were obtained using the same microscope but with a Photometrics cooled CCD camera and specific filter sets for NBD and Texas-Red as described in Mayor et al. (1993). Recycling compartments were identified as described above except that all spots greater than 30 pixels were retained and the two sets of images were analyzed separately. The width of one pixel was equivalent to 0.21 μm when a 40× objective was used with the cooled CCD camera. In all cases the recycling compartment colocalized with the two different labels. Typically, six random fields were measured for each dish. Tx-Tf and C_6-NBD-SM fluorescence powers in the recycling compartment were summed and normalized to the total number of nuclei counted in phase images of these same fields.

Results

Sorting of Tf from LDL and Subsequent Transit to Recycling Compartment

Efflux of ^{125}I-Tf from 12–4 cells is slowed to 55% of the pa-

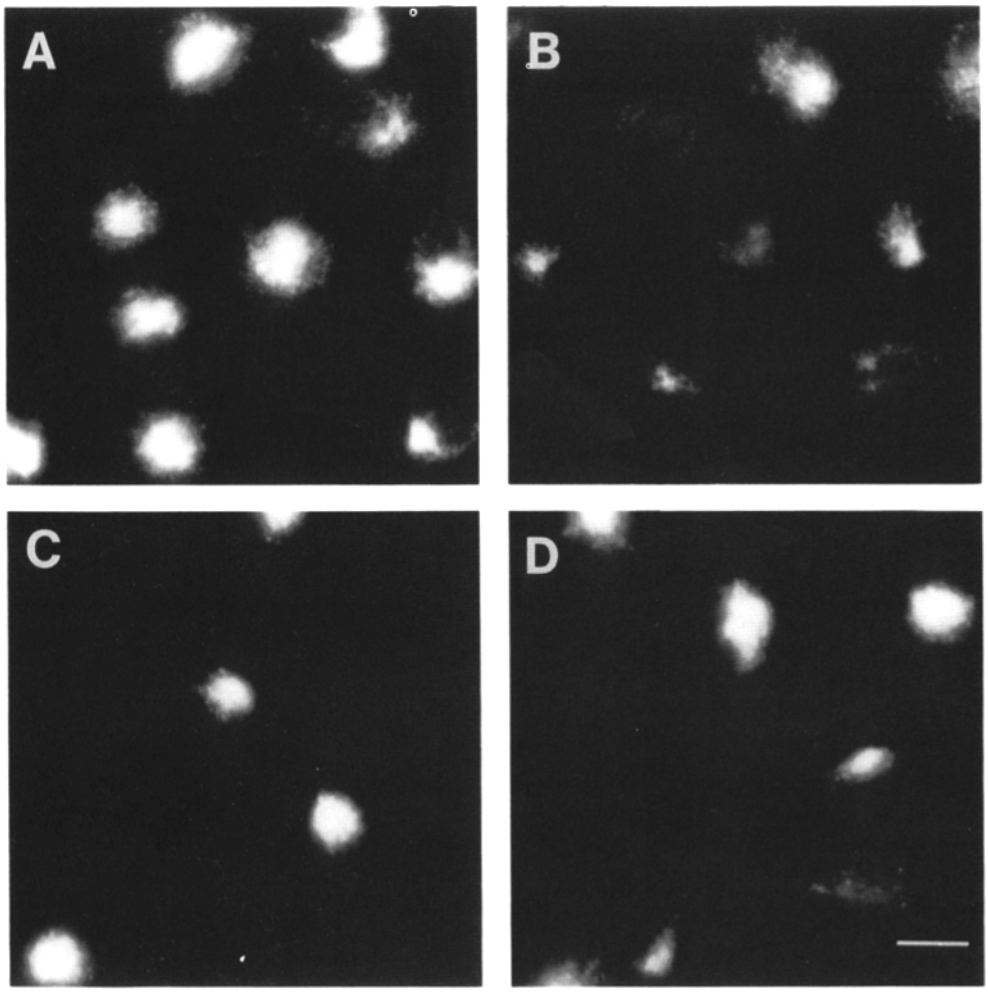

Figure 2. Exit of fluorescent Tf from mutant and parental cells. Parental TRVb-1 cells (*A*, *B*) and mutant 12–4 cells (*C*, *D*) were labeled with Tx-Tf (10 min), and chased for 6 min (*A*, *C*) or 18 min (*B*, *D*) in the absence of label as described in Materials and Methods. The bright spots are peri-centriolar recycling compartments similar to those in Fig. 1 *F*. Fluorescence images were obtained using a 40× objective and cooled CCD camera. Bar, 10 μm.

rental value (Johnson et al., 1993; Table I). To identify the affected step in Tf recycling, we studied the sequential steps starting with exit from the sorting endosome. LDL and Tf are initially delivered to sorting endosomes together, and they are then rapidly sorted into separate populations of endosomes that traffic to different destinations. Sorting of Tf from LDL was compared in mutant and parental cells. Cells were pulsed for 2 min with a mixture of DiI-LDL and FITC-Tf and colocalization of Tf and LDL was assayed after various chase times in the absence of fluorescent ligands. In 12–4 cells, Tf and LDL are initially colocalized, showing that they are internalized into the same sorting endosomes (Fig. 1, *A* and *B*). After a 4-min chase (Fig. 1, *C* and *D*), Tf is mostly not colocalized with LDL. By 8 min (Fig. 1, *E* and *F*), the separation is essentially complete, and Tf is in the peri-centriolar recycling compartment while LDL is in vesicles that are devoid of FITC-Tf. Tf was delivered to the peri-centriolar recycling compartment in TRVb-1 cells with similar kinetics (Fig. 1, *D* and *F*; Dunn et al., 1989; data not shown). Thus, the kinetics and morphology of Tf trafficking in the early portions of the Tf recycling pathway appear normal, and any defects that may be present in these steps do not account for the slowed total recycling kinetics of Tf in the mutant cells.

Exit of Tf From the Recycling Compartment is Slowed in Mutant Cells

To observe exit of Tf from the recycling compartment, cells were incubated with Tx-Tf to label Tf receptors in endocytic compartments. The localization of Tf is similar in the mutant and parental cells at the end of the labeling period with the majority of the intracellular fluorescence in the peri-centriolar recycling compartment. Fig. 2, *A* and *C*, show a similar pattern in parental and mutant cells that were pulsed for 10 min, and then chased for 6 min (to clear sorting endosomes). When cells were chased for 18 min in the absence of fluorescent Tf, much of the Tf was cleared from the parental cell (Fig. 2 *B*). However, the recycling compartments of 12–4 cells remain strongly labeled after the 18-min chase (Fig. 2 *D*).

Because most of the intracellular Tf is in a compact network of tubules and vesicles near the centrioles and the Golgi apparatus (Yamashiro et al., 1984; Fig. 1 *F*), it is imaged as a single contiguous labeled area by fluorescence microscopy (Fig. 2). By measuring the fluorescence power in this structure, it is possible to quantify the rate of exit of Tf from the recycling compartment on a single cell basis. Cells were labeled with a mixture of FITC-Tf and TRITC-Tf to steady

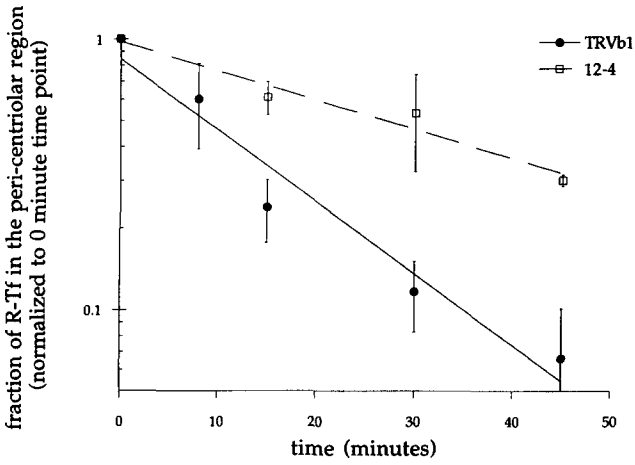

Figure 3. Exit of fluorescent Tf from peri-centriolar recycling endosomes in mutant and parental cells. Cells were labeled for 1 h with a mixture of FITC-Tf (10 μg/ml) and TRITC-Tf (10 μg/ml). They were chased for varying lengths of time in the presence of FITC-Tf (20 μg/ml) and fixed in 3.7% formaldehyde. In each experiment, fluorescein and rhodamine images of several fields were recorded with an image intensified video camera using a 40× objective. These images were digitized, and the central recycling compartment of each cell was identified and quantified to determine the fraction of TRITC-Tf remaining at that time, as described in Materials and Methods. In each experiment, results were normalized so that the value for TRITC-Tf at 0 min was 1.00. Each data point is the average of three experiments ± SD.

state for 1 h. The cells were then chased in the presence of FITC-Tf alone for varying lengths of time and fixed. By measuring the fluorescein/rhodamine ratio in the large spot corresponding to the recycling compartment, the mole fraction of total receptors labeled with TRITC-Tf was determined at different chase times on a cell-by-cell basis. Rate constants were determined from the mean of three independent experiments in parental and mutant cells.

As shown in Fig. 3, Tf left the recycling compartment of TRVb-1 cells with a rate constant of 0.062 ± 0.014 min^{-1}, while the rate for exit from the recycling compartment of 12–4 cells was 0.025 ± 0.001 min^{-1}. Thus, exit of Tf from the recycling compartment is slowed in the mutant cells as compared to the parental cell line. This difference in kinetics of exit from the recycling compartment is sufficient to account for the overall difference in recycling rate.

C_6-NBD-SM Exits the Recycling Compartments of Parental and Mutant Cells at Similar Rates

C_6-NBD-SM is internalized nonselectively as a bulk membrane marker, and uninternalized C_6-NBD-SM can then be efficiently back-exchanged from the cell surface (Koval and Pagano, 1989, 1990). Internalized C_6-NBD-SM colocalizes with Tf in the recycling compartment of TRVb-1 cells (Koval and Pagano, 1989), and, once internalized, recycles to the cell surface with identical kinetics to the Tf-R (Mayor et al., 1993). We have compared C_6-NBD-SM and Tf-R recycling in 12–4 and TRVb-1 cells, using both biochemical and quantitative light microscopic techniques.

Cells were allowed to internalize prebound Tx-Tf and C_6-NBD-SM at 37°C for 10 min. C_6-NBD-SM and Tx-Tf were then removed from the surface by back exchange on ice as described in Materials and Methods. Cells were then returned to 37°C, and chased in the presence of a back-exchange buffer (1% BSA in medium 1) for varying lengths of time. The distribution of C_6-NBD-SM and Tx-Tf in 12–4 cells after 6 or 18 min chase is shown in Fig. 4. Comparing the 6 min chase (Fig. 4, *A* and *C*) to the 18 min chase (Fig. 4, *B* and *D*), it can be seen that C_6-NBD-SM exits 12–4 cells more rapidly than Tf. This in contrast to the parental cells, in which Tx-Tf and C_6-NBD-SM are lost at the same rates (Mayor et al., 1993).

Quantitative analysis of the exit of C_6-NBD-SM and Tf from the peri-centriolar recycling compartment of mutant cells is shown in Fig. 5. In these cells, the rate of exit of Tx-Tf is only ~40% of the rate of exit of C_6-NBD-SM from the recycling compartment. The rate constants are shown in Table I along with data from Johnson et al. (1993) on the comparable rates in the parental line. C_6-NBD-SM exits the recycling compartment in 12–4 cells at a rate that is indistinguishable from the rates at which both C_6-NBD-SM and Tx-Tf exit in the parental cell line. These data show that while the rate of Tf exit from the recycling compartment of 12–4 cells is slowed 2–2.5-fold with respect to the parental cell line, the rates of exit of C_6-NBD-SM from the two cell lines are indistinguishable.

To rule out the possibility that the enhanced rate of C_6-NBD-SM exit from 12–4 cells was a result of hydrolysis of C_6-NBD-SM to C_6-NBD-Cer and subsequent transport of the ceramide or resynthesized C_6-NBD-SM and/or C_6-NBD-glucosylceramide to the cell-surface via nonvesicular transport, TLC analysis of the total NBD-lipid in the cells and in the medium at each time point was carried out in separate dishes. Under the conditions of the experiment (10-min pulse to load cells with C_6-NBD-SM and periods of chase, up to 30 min), <5% of the total cellular NBD-lipid was metabolized to C_6-NBD-Cer. No C_6-NBD-glucosylceramide was detected (detection limits ~2–8% of total lipid at the various time points) ruling out the possibility that C_6-NBD-lipid fluorescence was leaving the cells via conversion to C_6-NBD-glucosylceramide from C_6-NBD-Cer at the Golgi apparatus (Futerman et al., 1990; Futerman and Pagano, 1991; Jeckel et al., 1990) and subsequent translocation to the cell surface via the secretory pathway. When TRVb-1 cells were labeled for 30 min with C_6-NBD-Cer, and then analyzed by TLC, the ratio of newly synthesized C_6-NBD-glucosylceramide to newly synthesized C_6-NBD-SM was found to be 0.58:1 (data not shown). The lack of detectable conversion to C_6-NBD-glucosylceramide also rules out any significant contribution of newly synthesized C_6-NBD-SM to the exit rate (Koval and Pagano, 1989).

The exit kinetics of C_6-NBD-SM from parental and mutant cells were also compared by directly measuring the amount of C_6-NBD-SM recycled to the cell surface and released into back exchange medium containing 1% BSA. Fig. 6 shows that the kinetics of C_6-NBD-SM exit from both cell lines are indistinguishable from each other. The data obtained are not fit well with a single exponential decay, but they do fit a double exponential decay. A fast component (rates of 0.25 min^{-1} for TRVb-1 cells and 0.29 min^{-1} for 12–4 cells) accounts for 27% (TRVb-1) or 23% (12–4) of the loss of C_6-NBD-SM, and a slower component (rates of 0.060 ± 0.1 min^{-1} for TRVb-1 cells, and 0.065 ± 0.01 min^{-1} for 12–4 cells) accounts for 73% (TRVb-1) or 77% (12–4)

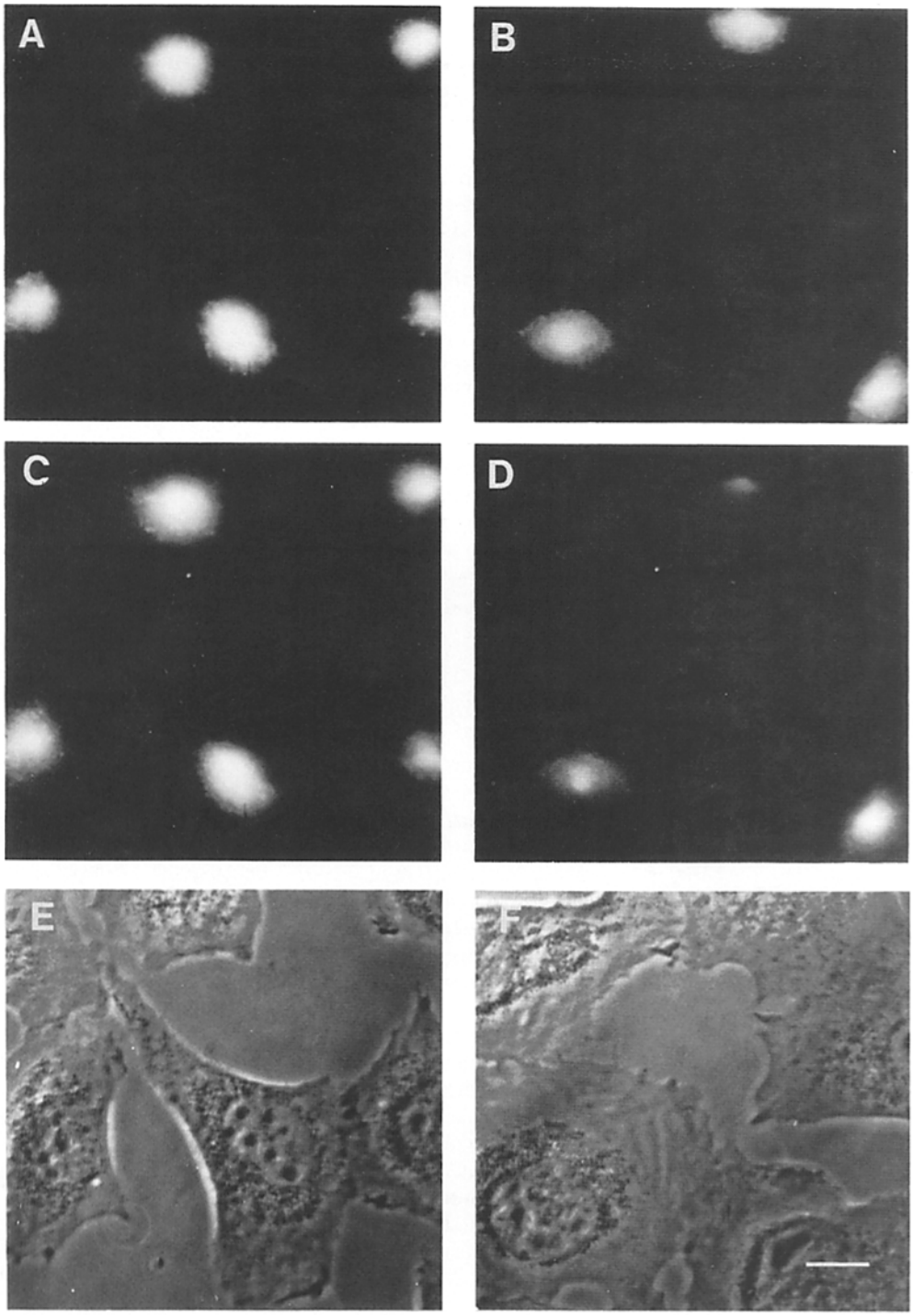

Figure 4. Exit of Tx-Tf and C_6-NBD-SM from 12–4 cells. Cells were labeled with Tx-Tf and 2.5 μM C_6-NBD-SM on ice as described in Materials and Methods. They were then warmed for 10 min to allow internalization of Tx-Tf and C_6-NBD-SM. Cells were chilled, and surface SM was removed by back exchange. The cells were then warmed to 37°C in medium 1 containing 1% BSA for the indicated lengths of time. Images shown were taken with a cooled CCD camera using a 40× objective. Tx-Tf (*A*, *B*) and C_6-NBD-SM (*C*, *D*) images were collected from the same field at 6 min (*A*, *C*) and 18 min (*B*, *D*) into the chase period. The corresponding phase contrast images of the cells chased for 6 min (*E*) or 18 min (*F*) are shown. Bar, 10 μm.

of the C_6-NBD-SM that is released into the medium. The nature of the fast component of release is not known at the present time. However, as shown in Table I, the slow component corresponds very closely to the rate of C_6-NBD-SM exit from the recycling compartment that was measured by quantitative fluorescence microscopy.

The pH of Endocytic Compartments

The pH of Tf-containing endosomes was measured by means of a confocal microscopic fluorescence emission ratio assay (see Materials and Methods). The narrow focal sectioning possible with confocal microscopy permits collection of fluorescent images of living cells in the presence of extracellular fluorescent ligand which obscures cellular fluorescence when using conventional wide-field microscopy. This capability is important for imaging sorting endosomes since Tf is rapidly removed from sorting endosomes (with a half-time of 2–3 min, Salzman and Maxfield, 1989; Dunn et al., 1989). Thus, in the absence of extracellular ligand, the sorting endosome is rapidly depleted of Tf.

In experiments in which cells were incubated in F-R-Tf for 10–40 min the median pH of peripheral Tf-containing com-

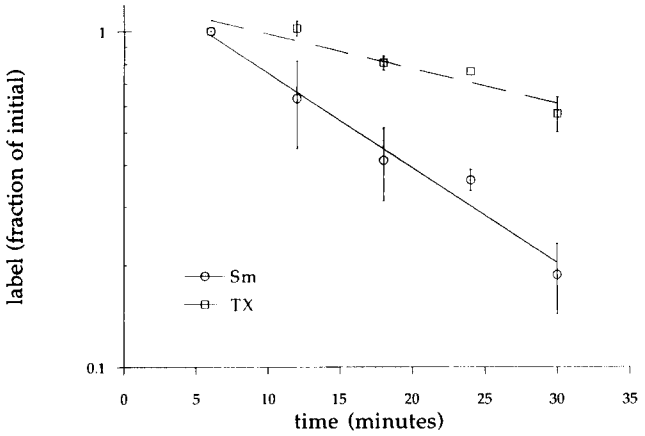

Figure 5. Exit of SM and Tf from recycling compartment. 12–4 cells were labeled for 10 min with a mixture of C_6-NBD-SM and Tx-Tf as described in Fig. 4. In each experiment, several fields (5–6) were analyzed for each time point, and the fluorescence from the central recycling compartment of each cell was identified and quantified as described in Materials and Methods. The sum of the C_6-NBD-SM and Tx-Tf fluorescence measured from the recycling compartments was divided by the total number of nuclei in each field. The values for Tx-Tf and C_6-NBD-SM were normalized to the 6 min time point. Each data point is the average of three experiments ± SD. Fields were selected randomly using phase contrast images.

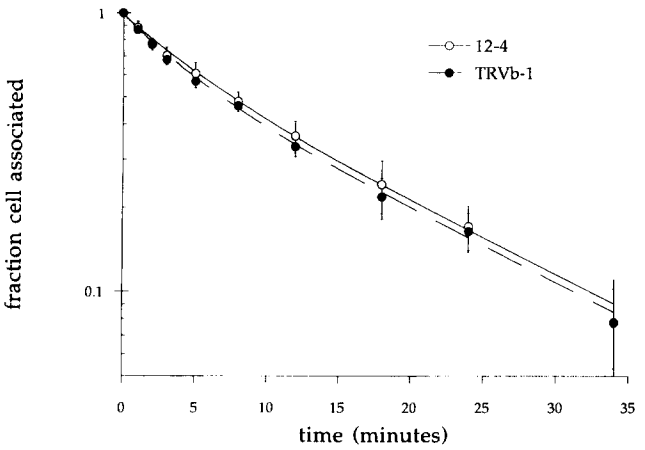

Figure 6. Exit of C_6-NBD-SM from TRVb-1 and 12–4 cells. TRVb-1 and 12–4 cells grown in 28 cm^2 dishes were labeled with 5 μM C_6-NBD-SM at 0°C for 30 min, and warmed up for 10 min at 37°C to allow internalization. C_6-NBD-SM remaining on the surface was then removed by back exchange at 0°C. Cells were then chased at 37°C in 4 ml of medium 1 containing 1% BSA. At the indicated times, 400-μl aliquots of chase medium were removed and replaced with 400 μl of prewarmed chase medium. NBD-lipid in the chase medium was measured by spectrofluorometry as described in Materials and Methods. At the end of the experiment, the remaining medium was removed and NBD fluorescence was measured. Finally, the cells were butanol extracted to determine cell-associated fluorescence and the fraction of cell associated lipid was determined as described in Methods. Each data point is an average of four experiments. Lipid in cells and medium at the end of the experiment was examined by TLC, and no metabolites of C_6-NBD-SM were found.

partments (presumably sorting endosomes) in TRVb-1 cells was 5.9–6.0, while the median pH for 12–4 cells was 6.4 to 6.5. Frequency distributions of rhodamine/fluorescein ratios in punctate endosomes for TRVb-1 cells and 12–4 cells incubated for 10–20 min are shown in Fig. 7 *B*. These results are consistent with those previously obtained by Yamashiro and Maxfield (1987) in studies of another *end*2 CHO cell line, DTF 1-5-1 cells, which showed that the pH of peripheral endosomes was more alkaline in DTF cells than in wild-type WTB cells.

The pH of the peri-centriolar recycling compartment was also found to be relatively alkaline in 12–4 cells. In one experiment, pH was measured between 30–40 min of labeling, and the mean pH of the recycling compartment of TRVb-1 cells was 6.43 ± 0.03 (SE, $N = 34$) while the mean pH of the recycling compartment of 12–4 cells was 6.67 ± 0.05 (SE, $N = 26$). In a separate experiment, pH was measured between 10–20 min of labeling, and the mean pH of the recycling compartment was 6.52 ± 0.02 (SE, $N = 52$) and 6.69 ± 0.05 (SE, $N = 27$) for TRVb-1 cells and 12–4 cells, respectively. Although the differences between cell lines are not large, they were analyzed by *t*-test and are statistically significant with a probability value of <0.05.

Discussion

12–4 cells are a clonal mutant CHO cell line that belongs to the *end*2 complementation group (Johnson et al., 1993). The *end*2 group has been shown to have several alterations in protein trafficking, which have been associated with changes in endosomal pH (Robbins et al., 1983, 1984; Schmid et al., 1989; Yamashiro et al., 1987). Because the 12–4 cells are derived from a CHO cell line, TRVb-1, which expresses the human transferrin receptor but no detectable hamster transferrin receptor, Johnson et al. (1993) were able to carry out kinetic studies of transferrin recycling with greater precision than had been achieved with other *end*2 lines. They found that Tf exits from 12–4 cells at 55% of the rate in TRVb-1 cells. The internalization rates of both Tf and LDL were also reduced, indicating that the defect affects multiple receptors and more than one step in the Tf-R recycling pathway. The slow release of Tf was not due to futile cycling of diferric-Tf as a consequence of impaired endosome acidification because very little diferric-Tf was detected on the cell surface. Furthermore, the recycling of unoccupied receptors was also slowed in the 12–4 cells (Johnson et al., 1993). Thus, the slow exit of Tf from 12–4 cells does not result from futile cycling of iron-loaded Tf through nonacidified endosomes, but it results directly from slow receptor recycling. In this study we examined the Tf recycling pathway step by step in 12–4 cells and the parental TRVb-1 cells to determine the site of the defect.

Transferrin Recycling

Transferrin and LDL enter early sorting endosomes together. In TRVb-1 cells, Tf sorts from LDL with a half-time of <3 min (Dunn et al., 1989; Salzman and Maxfield, 1989). We found that Tf sorted from the lysosomally directed LDL in 12–4 cells at a rate similar to that found in parental cells, with sorting completed by 8 min. Similarly, the rate of appearance of Tf in the recycling compartment was indistin-

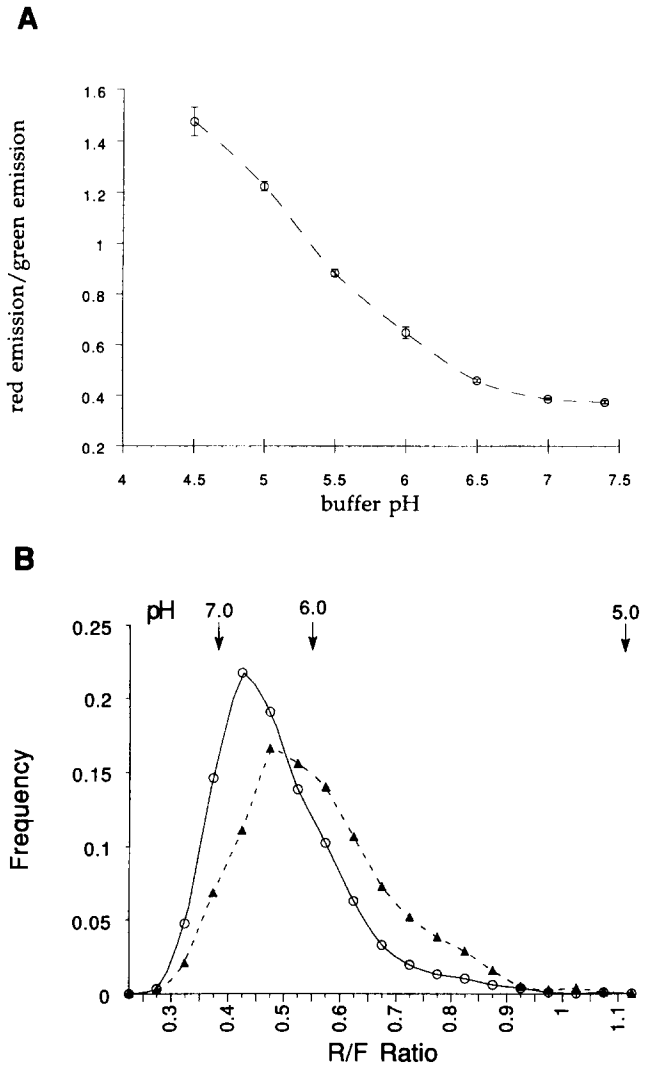

Figure 7. Endosome pH in TRVb-1 and 12–4 cells. (*A*). A representative F-R-Tf endosome pH calibration curve. Cells labeled for 5 min with F-R-Tf as described in the text, were fixed in 2% formaldehyde in medium 1 and equilibrated for >30 min in pH buffers with the indicated pH values plus 40 mM methylamine. Images were collected, and the rhodamine to fluorescein (*red/green*) fluorescence emission ratio was measured as described in Materials and Methods. Indicated values are SEM of six fields and represent a total of 150–650 endosomes each point. (*B*). Frequency distribution of punctate endosome fluorescein/rhodamine ratios for TRVb-1 cells (*triangles*) and 12–4 cells (*circles*) labeled for 10 min with 20 μg/ml F-R-Tf. Images were collected, and the ratios were calculated as described in Methods. These histograms represent the combined data of 12 fields each, representing a total of 2,967 endosomes for TRVb-1 cells and 2,787 endosomes for 12–4 cells.

guishable in the mutant and parental cell lines. Thus, Tf-R is removed from sorting endosomes and delivered to the recycling compartment normally. If there are any differences at all in these rates, they are too small to contribute significantly to the overall reduction in recycling rate.

Although entry into the recycling compartment is normal, exit from this compartment is slowed substantially in 12–4 cells. We used digital image processing to analyze the amount of Tf remaining in the central recycling compartment at different chase times in TRVb-1 and 12–4 cells. Tf exited the recycling compartment at a 2.5-fold slower rate in 12–4 cells than in TRVb-1 cells after labeling of the cells to steady state ($t_{1/2}$ 11.2 min for TRVb-1 vs 27.7 min for 12–4, Table I). Similar differences in the exit kinetics were seen after a short pulse with Tf and varying chase times (Fig. 5; Table I; and data not shown).

Bulk Membrane Recycling in Parental and 12–4 Cells

The studies we have described here depend on the ability to remove fluorescent probes only when they return to the cell surface by recycling. Tf does this naturally by conversion to apo-Tf which dissociates from the Tf-R upon exposure to neutral pH. Unfortunately, most fluorescent labels of recycling receptors either dissociate from receptors in endosomes or remain bound at the cell surface and re-enter the endocytic pathway, making it difficult to measure passage between internal compartments and back to the cell surface. However, a fluorescent lipid analog, C_6-NBD-SM, is very efficiently removed from the plasma membrane when lipid acceptors such as liposomes or albumin are in the chase medium (Koval and Pagano, 1989). Koval and Pagano (1989) have taken advantage of this property to show that nearly all internalized C_6-NBD-SM returns to the cell surface. Mayor et al. (1993) have shown that internalized C_6-NBD-SM and Tf move through each of the steps of the recycling pathway with essentially identical kinetics. These studies were carried out in two cell lines, TRVb-1 and WTB cells. WTB cells, a parental CHO cell line, recycle C_6-NBD-SM at a rate threefold faster than TRVb-1 cells, and they recycle the Tf-R at a rate that matches the rate of recycling of C_6-NBD-SM within an experimental error of <10%. Thus, in parental CHO cells, the Tf-R inside the cell moves in a manner similar to bulk membrane (i.e., efficient recycling is a default pathway in the parental cell lines).

In this study, we used C_6-NBD-SM as a probe of bulk membrane exit from the recycling compartment. If the defect in 12–4 cells were in overall membrane traffic out of the recycling compartment, we would expect exit of C_6-NBD-SM from this compartment to be affected to the same extent as Tf. In biochemical assays, we showed that the rate and overall kinetics of exit of C_6-NBD-SM were the same in 12–4 and parental cells. Furthermore, digital image analysis of cells labeled with both Tf and C_6-NBD-SM showed that exit of C_6-NBD-SM from the peri-centriolar recycling compartment in 12–4 cells was faster than Tf exit from the same cells, but similar to the rate of exit of Tf and lipid in parental cells. Thus, the flow of membrane from the recycling compartment occurs normally in 12–4 cells, but Tf-R are hindered in leaving with the bulk membrane. These differences in rate of exit of a membrane protein, the transferrin receptor, and a bulk membrane lipid show that the recycling compartment can act as a sorting organelle and not just as a passive reservoir of membrane proteins on the recycling pathway back to the cell surface.

Relationship to the Phenotype of End2 Cells

Several members of the *end2* complementation group have been isolated and characterized. They show increased resistance to diphtheria toxin, altered kinetics of iron uptake by transferrin, and defects in delivery of lysosomal enzymes to lysosomes (Robbins et al., 1983, 1984; Roff et al., 1986).

Many of these defects could be ascribed to a defect in endosomal acidification, and that has been suggested as the basis for many of the properties of *end2* cells. Endosomes isolated from different *end2* cell lines have reduced capability for ATP-dependent acidification (Schmid et al., 1989; Roff et al., 1986). As shown in Fig. 7, the pH of punctate sorting endosomes is higher on the average in the 12–4 cells than in the parental line. There was also a small but statistically significant difference in the pH values measured for pericentriolar recycling compartments. In two experiments, the differences between the average pH values for the recycling compartments in the two cell lines were 0.17 and 0.24 pH units.

The pH values found for the sorting endosomes span a range which is known to have effects on receptors and ligands (Maxfield and Yamashiro, 1991). In contrast, the pH range covered by the recycling compartments (~6.4–6.7) is relatively narrow. Thus, the slowed exit of transferrin from the recycling compartment may not be directly caused by an altered pH in that compartment. It is possible that an acidification defect elsewhere (e.g., in sorting endosomes) could lead to a defect in exit of transferrin from the recycling compartment. For example, altered pH in sorting endosomes could change the delivery of some components to the recycling compartment, and this could cause retention of Tf.

An alternative explanation of the acidification phenotype is that the alteration in endosome pH is secondary to a membrane protein trafficking defect. The pH in endosomes is maintained by a multisubunit electrogenic proton pump along with other ion transporters that control the electrical potential across the membrane (Al-Awqati, 1989; Barasch et al., 1991; Cain et al., 1991; Fuchs et al., 1989). A trafficking defect could lead to incorrect location or assembly of proton pumps, chloride channels, or other factors required for correct endosomal pH (Al-Awqati, 1989).

In this study we have demonstrated that the defect in transferrin receptor recycling can be accounted for entirely by a decreased rate of exit from the recycling compartment. Although the *end2* mutants have been considered to have their properties explained by a defect in pH regulation, this defect in recycling occurs in an organelle in which a relatively small acidification defect was measured. In the same mutant cells, there was no decrease in the rate of exit of a bulk membrane probe. Thus, the effect of the mutation was not on constitutive exit of membrane from the organelle, but rather it was a selective effect on trafficking of the Tf-R.

This retention of Tf-R relative to bulk membrane means that the recycling compartment is functioning as a sorting organelle. The molecular basis for retention of Tf-R in 12–4 cells is not known. It is possible that the 12–4 cells use a retention mechanism that is normally inactive in CHO cells or one that does not normally retain Tf-R. Retention of the Tf-R in the recycling compartment might then involve a similar mechanism to that involved in the retention of the GLUT4 glucose transporter in muscle or fat cells not exposed to insulin (Piper et al., 1992). We have been unable to measure accurately the exit rate of other proteins from the recycling compartment, so we do not know if there is selectivity in the retention of some membrane proteins. Nevertheless, the properties of the 12–4 mutant cell line demonstrate that the recycling compartment is not always a passive step in the recycling pathway. This compartment can play an active role in the sorting of membrane components. This defines a new set of possible functions for this organelle.

This work was supported in part by National Institutes of Health (NIH) grant DK27083 to F. R. Maxfield, and CA09503-08 to J. F. Presley, and American Cancer Society grants IN-77 and CG-8 to T. E. McGraw. S. Mayor was supported by a fellowship from the Helen Hay Whitney Foundation. L. S. Johnson was supported by an American Liver Foundation Student Fellowship and the NIH Medical Scientist Training Program.

Received for publication 17 March 1993 and in revised form 11 June 1993.

References

Al-Awqati, Q. 1989. Regulation of membrane transport by endocytotic removal and exocytotic insertion of transporters. *Methods Enzymol.* 172:49–59.

Barasch, J., B. Kiss, A Prince, L. Saiman, D. Gruenert, and Q. Al-Awqati. 1991. Defective acidification of intracellular organelles in cystic fibrosis. *Nature (Lond.).* 352:70–83.

Cain, C. C., R. B. Wilson, and R. F. Murphy. 1991. Isolation by fluorescence-activated cell sorting of Chinese hamster ovary cell lines with pleiotropic temperature-conditional defects in receptor recycling. *J. Biol. Chem.* 11746–11732.

Colbaugh, P. A., C.-Y. Kao, S.-P. Shia, M. Stookey, and R. K. Draper. 1988. Three new complementation groups of temperature-sensitive Chinese hamster ovary cell mutants defective in the endocytic pathway. *Somatic Cell Mol. Genet.* 14:499–507.

Dunn, K. W., and F. R. Maxfield. 1990. Use of fluorescence microscopy in the study of receptor-mediated endocytosis. *In* Noninvasive Techniques in Cell Biology. S. Grimstein and L. K. Foskett, editors. Wiley-Liss, Inc., New York. 153–176.

Dunn, K. W., T. E. McGraw, and F. R. Maxfield. 1989. Iterative fractionation of recycling receptors from lysosomally destined ligands in an early sorting endosome. *J. Cell Biol.* 109:3303–3314.

Fuchs, R., S. Schmid, and I. Mellman. 1989. A possible role for Na^+, K^+-ATPase in regulating ATP-dependent endosome acidification. *Proc. Natl. Acad. Sci. USA.* 86:539–543.

Futerman, A. H., and R. E. Pagano. 1991. Determination of the intracellular sites and topology of glucosylceramide synthesis in rat liver. *Biochem. J.* 280:295–302.

Futerman, A. H., B. Stieger, A. L. Hubbard, and R. E. Pagano. 1990. Sphingomyelin synthesis in rat liver occurs predominantly at the *cis* and medial cisternae of the Golgi apparatus. *J. Biol. Chem.* 265:8650–8657.

Goldstein, J. L., S. K. Basu, and M. S. Brown. 1983. Receptor mediated endocytosis of low-density lipoprotein in cultured cells. *Methods Enzymol.* 98:241–260.

Goldstein, J. L., M. S. Brown, R. G. W. Anderson, D. W. Russell, and W. J. Schneider. 1985. Receptor mediated endocytosis: concepts emerging from the LDL receptor system. *Annu. Rev. Cell Biol.* 1:1–39.

Harford, J. B., J. L. Casey, D. M. Koeller, and R. D. Klausner. 1991. Structure, function and regulation of the transferrin receptor: insights from molecular biology. *In* Intracellular Trafficking of Proteins. C. J. Steer and J. A. Hanover, editors. Cambridge University Press, New York. 302–334.

Hicke, L., and R. Schekman. 1990. Molecular machinery required for protein transport from the endoplasmic reticulum to the Golgi complex. *Bioessays.* 12:253–258.

Jeckel, D., A. Karrenbauer, R. Birk, R. R. Schmidt, and F. Wieland. 1990. Sphingomyelin is synthesized in the cis Golgi. *FEBS (Fed. Eur. Biochem. Soc.) Lett.* 261:155–157.

Johnson, L. S., J. F. Presley, J. C. Park, and T. E. McGraw. 1993. Slowed receptor trafficking in mutant CHO lines of the *end1* and *end2* complementation groups. *J. Cell Physiol.* In press.

Koval, M., and R. E. Pagano. 1989. Lipid recycling between the plasma membrane and intracellular compartments: transport and metabolism of fluorescent sphingomyelin analogs in cultured fibroblasts. *J. Cell Biol.* 108: 2169–2181.

Koval, M., and R. E. Pagano. 1990. Sorting of an internalized plasma membrane lipid between recycling and degradative pathways in normal and Niemann-Pick, type A fibroblasts. *J. Cell Biol.* 111:420–432.

Maxfield, F. R. 1989. Measurement of vacuolar pH and cytoplasmic calcium in living cells using fluorescence microscopy. *Methods Enzymol.* 173: 745–771.

Maxfield, F. R., and K. W. Dunn. 1990. Studies of endocytosis using image intensification fluorescence microscopy and digital image analysis. *In* Optical Microscopy for Biology. B. Herman and K. Jacobsen, editors. Wiley-Liss, Inc., New York. 357–371.

Maxfield, F. R., and D. J. Yamashiro. 1991. Acidification of organelles and the intracellular sorting of proteins during endocytosis. *In* Intracellular Trafficking of Proteins. C. J. Steer and J. A. Hanover, editors. Cambridge University Press, New York. 157–182.

Mayor, S., J. Presley, and F. R. Maxfield. 1993. Sorting of membrane compo-

nents from endosomes and subsequent recycling to the cell surface occurs by a bulk flow process. *J. Cell Biol.* 121:1257–1269.

McGraw, T. E., K. W. Dunn, and F. R. Maxfield. 1993. Isolation of a temperature-sensitive variant CHO cell line with a morphologically altered recycling compartment. *J. Cell Physiol.* 155:579–594.

McGraw, T. E., and F. R. Maxfield. 1990. Human transferrin receptor internalization is partially dependent upon an aromatic amino acid on the cytoplasmic domain. *Cell Regulation.* 1:369–377.

McGraw, T. E., L. Greenfield, and F. R. Maxfield. 1987. Functional expression of the human transferrin receptor cDNA in Chinese hamster ovary cells deficient in endogenous transferrin receptor. *J. Cell Biol.* 105:207–214.

Newman, A. P., and S. Ferro-Novick. 1990. Defining components required for transport from the ER to the Golgi complex in yeast. *Bioessays.* 12:485–491.

Novick, P., C. Field, and R. Schekman. 1980. Identification of 23 complementation groups required for post-translational events in the yeast secretory pathway. *Cell.* 21:205–215.

Novick, P., S. Ferro, and R. Schekman. 1981. Order of events in the yeast secretory pathway. *Cell.* 25:461–469.

Piper, R. C., C. Tai, J. W. Slot, C. S. Hahn, C. M. Rice, H. Huang, and D. E. James. 1992. The efficient intracellular sequestration of the insulin-regulatable glucose transporter (GLUT-4) is conferred by the NH2 terminus. *J. Cell Biol.* 117:729–743.

Robbins, A. R., C. Oliver, J. L. Bateman, S. S. Krag, C. J. Galloway, and I. Mellman. 1984. A single mutation in Chinese hamster ovary cells impairs both Golgi and endosomal functions. *J. Cell Biol.* 99:1296–1309.

Robbins, A. R., S. S. Peng, and J. L. Marshall. 1983. Mutant Chinese hamster ovary cells pleiotropically defective in receptor-mediated endocytosis. *J. Cell Biol.* 96:1064–1071.

Roff, C. F., R. Fuchs, I. Mellman, and A. R. Robbins. 1986. Chinese hamster ovary cell mutants with temperature-sensitive defects in endocytosis. I. Loss of function on shifting to the nonpermissive temperature. *J. Cell Biol.* 103: 2283–2297.

Salzman, N. H., and F. R. Maxfield. 1988. Intracellular fusion of sequentially formed endocytic compartments. *J. Cell Biol.* 106:1083–1091.

Salzman, N. H., and F. R. Maxfield. 1989. Fusion-accessibility of endocytic compartments along the recycling and lysosomal endocytic pathways in intact cells. *J. Cell Biol.* 109:2097–2104.

Schmid, S., R. Fuchs, M. Kielian, A. Helenius, and I. Mellman. 1989. Acidification of endosome subpopulations in wild-type Chinese hamster ovary cells and temperature-sensitive acidification-defective mutants. *J. Cell Biol.* 1989:1291–1300.

Tabas, I., S. Lim, X.-X. Xu, and F. R. Maxfield. 1990. Endocytosed βVLDL and LDL are delivered to different intracellular vesicles in mouse peritoneal macrophages. *J. Cell Biol.* 111:929–940.

Yamashiro, D. J., and F. R. Maxfield. 1987. Acidification of morphologically distinct endosomes in mutant and wild-type Chinese hamster ovary cells. *J. Cell Biol.* 105:2723–2733.

Yamashiro, D. J., B. Tycko, S. R. Fluss, and F. R. Maxfield. 1984. Segregation of transferrin to a mildly acidic (pH 6.5) para-Golgi compartment in the recycling pathway. *Cell.* 37:789–800.